



Article

Biological Machine Learning Combined with *Campylobacter* Population Genomics Reveals Virulence Gene Allelic Variants Cause Disease

DJ Darwin R. Bandoy^{1,2} and Bart C. Weimer^{1,*}

¹ 100 K Pathogen Genome Project, Department of Population Health and Reproduction, School of Veterinary Medicine, University of California Davis, Davis, CA 95616, USA

² Department of Veterinary, Paraclinical Sciences, College of Veterinary Medicine, University of the Philippines Los Baños, Los Baños 4031, Philippines; drbandoy@ucdavis.edu

* Correspondence: bcweimer@ucdavis.edu; Tel.: +1-530-760-9550

Received: 3 March 2020; Accepted: 8 April 2020; Published: 10 April 2020



Abstract: Highly dimensional data generated from bacterial whole-genome sequencing is providing an unprecedented scale of information that requires an appropriate statistical analysis framework to infer biological function from populations of genomes. The application of genome-wide association study (GWAS) methods is an appropriate framework for bacterial population genome analysis that yields a list of candidate genes associated with a phenotype, but it provides an unranked measure of importance. Here, we validated a novel framework to define infection mechanism using the combination of GWAS, machine learning, and bacterial population genomics that ranked allelic variants that accurately identified disease. This approach parsed a dataset of 1.2 million single nucleotide polymorphisms (SNPs) and indels that resulted in an importance ranked list of associated alleles of *porA* in *Campylobacter jejuni* using spatiotemporal analysis over 30 years. We validated this approach using previously proven laboratory experimental alleles from an in vivo guinea pig abortion model. This framework, termed μ PathML, defined intestinal and extraintestinal groups that have differential allelic *porA* variants that cause abortion. Divergent variants containing indels that defeated automated annotation were rescued using biological context and knowledge that resulted in defining rare, divergent variants that were maintained in the population over two continents and 30 years. This study defines the capability of machine learning coupled with GWAS and population genomics to simultaneously identify and rank alleles to define their role in infectious disease mechanisms.

Keywords: *porA*; infectious disease; XGBoost; *Campylobacter*; abortion; protein modeling; artificial intelligence; allelic variation; bacterial metastasis

1. Introduction

Comparative microbial genomics has relied on pangenome comparisons to characterize changes in the core and flexible genome, which provided genes lists associated with gene changes but had little association with determine the causal genes for a disease [1]. An alternative approach to this perspective is the use of genome-wide association (GWAS) analyses, which are commonly used in mammalian genomics, in an effort to refine the estimates of specific genes of interest for microbial gene association with phenotype, such as pathogenicity. However, a limitation of GWAS is the sequential examination of single loci, which prevents simultaneous analysis of multiple genes or allelic variants that may interact to cause a phenotype. This is a severe limitation in comparative bacterial genomics, especially as the population of bacterial genomes continues to grow reaching nearly 1 million in With this large number of genomes that often represent multiple genomes for a single species or serotype, it is appropriate to treat each genome as a member of a population of individuals that are

spatiotemporally distributed. A spatiotemporal analysis framework makes it possible to examine the non-linear evolutionary rates of each genome in combination with specific selective conditions for all of the alleles of specific genes found in very large populations that are maintained or diluted in populations that are consistently associated with microbial phenotypes—especially disease and tissue tropism. However, this approach adds to an ever-growing big data problem for microbial genomics requiring new approaches for microbial comparative genomics and statistical methods. To address these limitations with highly dimensional bacterial genome analyses, we can use the integration of multidimensional metadata alongside the strain differences to create a robust analysis framework that can be used with GWAS [2].

A compounding limitation of this framework is the lack of appropriate statistical models that underpin this approach in bacteria since it is unknown when the populations are normally distributed or evolving non-linearly. As with all big data problem sets, the multiple comparisons problem requires a correction, such as the Bonferroni correction, to adjust the p -value, which moves this correction to problems that are beyond what was contemplated when this approach was invented for gene expression (Table 1) [3]. Further, the assumption that each gene or allele behaves independently within the genome is conceptually flawed in bacteria considering the operon configuration, horizontal gene transfer (e.g., plasmids), and the evolution rate of bacteria are on the order of minutes rather than years in mammals. Hence, alternative analyses that are biological and statistically compatible need to be defined for bacterial population genomics.

Table 1. Exemplar comparison of statistical metrics of genome-wide association study (GWAS) versus machine learning metrics. Allelic variant association with phenotype using XGBoost. An allele can be very large, ~8000 for *porA* for a pairwise comparison. Using a population of this gene from 200 genomes created a population variation of 1.2 million variants that can be ranked with an estimation of importance to association with the disease phenotype, abortion in this case.

Allele	GWAS Statistical Metrics		Machine Learning Coupled to GWAS Metrics	
	GWAS p -Value	Bonferroni Corrected p -Value	Candidate Ranking	Feature Importance
X_1	0.001	8.3×10^{-10}	1	80
X_2	0.001	8.3×10^{-10}	2	75
X_3	0.001	8.3×10^{-10}	3	70
X_n	0.001	8.3×10^{-10}	Rank _{n}	Importance _{n}

Coupling GWAS, population microbial genomics, and machine learning is poised to be a robust alternative to classical GWAS or pangenome comparisons alone; however, the combination of these methods will likely simultaneously discover changes in microbial genomes and gene variation that span the spatiotemporal scale, genome plasticity, and large numbers of selection conditions that result in gene variation that maybe causal in disease but with only a subset of gene variants or specific alleles with cause variation in the disease symptoms. Moreover, this combination (coined here as μ PathML) produces a statistically valid method that results in biologically informative rankings for each genome, gene, and allele that are not determined from any of the individual analyses alone. These advantages, combined with downstream inspection of the prioritized rankings, further power biological discovery to bring insightful observations about the genome and the phenotype, especially when large genome populations are used in the analysis, from very divergent populations of alleles. To extend this concept, highly divergent sequences with similar function that are missed with automated gene calling approaches can be brought back into biological relevance, especially if gene mutations are tracked as new genes as was done by Weimer et al. [4] and Kaufman et al. [5–7].

An analytical strength of machine learning for use in microbiology is the ability to define functional relationships from population-scale genome comparisons or genes without a priori definition of the underlying mechanism of change or specific phenotype limitations [8]. This distinctive advantage makes machine learning superior to classical statistical tests for microbial applications because the

individual genomes are so highly variable in gene content and phenotypes that lead to varying displays of the disease and tissue location [9,10]. This is particularly useful in bacteria when causal genes act in combination or do not evolve linearly, gene variants interact, varying evolutionary rates between genes within the same genome, or assumptions of normal distribution are violated in part due to the selection conditions [2,11]. These biological conditions and parameters are incompatible with the assumptions of linear or correlative statistics, which is compounded with data reduction methods, which provide a very small snapshot of the genome variation that yield associations with low predictive value that is compounded by highly variable genomes of the same species [12–15], such as with microorganisms.

2. Materials and Methods

2.1. Biological Feature Engineering

Biological feature engineering entails selection of pertinent controls and cases for μ PathML analysis. The genomes between gastrointestinal and extraintestinal abortive isolates. *Campylobacter jejuni* controls were downloaded from Patric 3.5.28 (<https://www.patricbrc.org/>), 1 June 2019 (Table S2). Abortive extraintestinal genomes of *C. jejuni* were obtained from the Sequence Read Archive (SRA; Table S3) [16]. Fastq files were assembled using Shovill (version 1.0.4; <https://github.com/tseemann/shovill>). Assembled files were annotated with Prokka (version 1.13.3) [17]. Variant calling was done with the reference sequence *C. jejuni* NTC11168 with Snippy (version 4.3.5; <https://github.com/tseemann/snippy>) as previously described [18].

2.2. Gradient Tree Boosting as GWAS Framework

GWAS variants generated from the biological feature engineering step were used as input for XGBoost. The original source code for implementing gradient tree boosting is available at <https://xgboost.readthedocs.io/>. A confusion matrix was generated and used to assess the performance of the model (Table S4). The relative importance of the predictive model was used as the GWAS hits.

2.3. Tetris Plot

Classical GWAS hits are displayed as the negative logarithm of the p -value in Manhattan plots, hence we formulated a novel visualization of the ranked alleles generated by the machine learning model to highlight the difference between approaches—we call this GWAS hit visualization a Tetris plot and used when color coding the relative importance values of the associated alleles derived from the XGBoost (green being associated and red being non-associated). The source genome is plotted on the y -axis and genomic coordinates on the x -axis overlaid with a GWAS hits presence or absence matrix.

2.4. Population-Wide Whole-Genome Phylogeny

The genome distance metric was calculated using genome-wide k-mer signatures to generate the population-wide phylogeny with a k-mer size of 31 scaled to 1000 with Sourmash [19]. The resulting genome-wide k-mer distance was visualized as an all-against-all heatmap [19].

2.5. Protein Modeling

Assembled genomes were annotated using Prokka (Version 1.13.3) and PorA protein sequences were extracted for protein modeling using Swiss Model [20,21]. The most homologous protein was used as template for protein modeling. Illustrate (<https://ccsb.scripps.edu/illustrate/>) was used to generate the protein visualization of the alleles. Ranked BioML alleles identified by visual inspection of the Tetris plot, via the ranked variable importance were used to inspect the protein structures.

3. Results

In this study, we coupled GWAS with machine learning and population bacterial genomics (Figure 1) creating a broadly applicable framework that was validated using previously published

verified alleles of a virulence gene that causes abortion in livestock [16,22,23]. We hypothesized that specific alleles of a single gene (i.e., *porA*) define the ability of *Campylobacter* for extraintestinal invasion and further are causative of abortion with specific alleles. This was done using a wet-lab validated data set containing 100 genomes [16,22,23] combined with machine learning using extreme gradient boosting (XGBoost) [24,25]. The ability to interrogate the predictive features emerged as a tool to determine mechanistic function in complex biological systems [26]. XGBoost implements adaptive optimization within the functional space by iteration of the weak learners into strong learners represented by decision trees, where each new decision tree is generated by factoring the residuals generated from the difference from the observed to the predicted feature (Figure 2; Table S1).

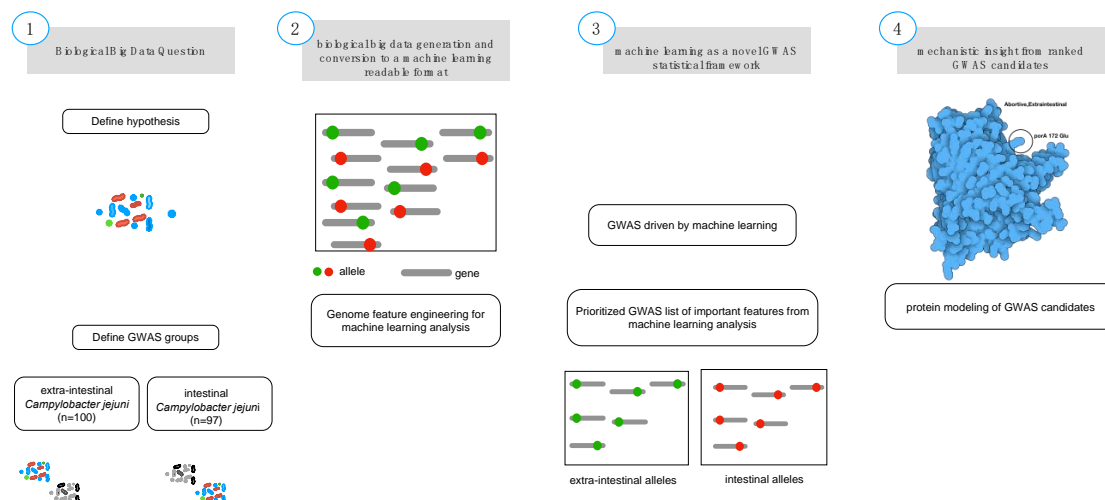


Figure 1. Biological feature engineering of genomic data for machine learning analysis. A critical step in feature engineering is selection of the appropriate comparison groups to enable classification of alleles that are related to the specific phenotype of interest (i.e., intestinal (controls; diarrheal; $n = 108$) and extraintestinal (cases; abortive; $n = 85$) (Step 1). Population-wide allelic variants (red dot = intestinal, green dot = extraintestinal) that result from variant calling (Step 2) and are used as the input features for machine learning analysis (Step 3). The predicted model generated from the machine learning analysis is inspected for the most predictive features using biological context, input, and protein modeling (Step 4) that represents a non-synonymous mutation from the genomic population of allelic variants ($n = 193$).

We used previously validated wet-lab data with a tetracycline-resistant strain of *C. jejuni* causing abortion in sheep [16,22,23] as the validation training set for μ PathML analysis. Previously, these robust studies used a pairwise comparison to identify 8000 single nucleotide differences (SNP) differences between a reference genome and an abortive strain that subsequently utilized genetically transformed genomes to identify specific allelic variants that cause abortion in a model system. We validated μ PathML using 85 genomes that span 30 years and multiple locations as a reference set of cases and 108 control genomes of intestinal and diarrheal isolates. This approach permitted exploration of the bacterial population genomic space of this organism by linking different phenotypes to validated genome variation (Figure 1). Biological feature engineering of this collection identified 1.2 million SNPs, which is not tractable using in vivo infection studies, to determine the role of all SNPs in this gene across the bacterial population to cause this disease. To use this approach at a big-data scale, we hypothesized that genomic changes evolved in gastrointestinal *C. jejuni* resulting in an abortive phenotype; hence, invading the intestine and progressing to other tissues—in this case the placenta resulting in abortion. Applying μ PathML analysis to the population of gastrointestinal, diarrheal *C. jejuni* versus extraintestinal, abortive phenotypes produced a ranked set of alleles in a ranked order of importance to the phenotype (i.e., abortion) (Table S1).

μ PathML analysis identified 14 *porA* loci as the most important alleles ranging from 1.0 to 0.65 scaled importance out of the 1.2 million SNPs (Table S1). These ranked loci were compared by body location (Figure 3), which further clarified the location of these SNPs and indels that simultaneously presented the ranked associated allelic variants within the phenotype of interest as detected with μ PathML as well as the non-associated alleles. This analysis method enabled modeling of various protein structures for PorA between abundant versions to hybrid variation and rare variants that were not captured by automated gene calling, machine learning alone, or classical statistical testing. Regions within *porA* from the cases expressing different allelic versions were further explored for each genome and ranked *porA* allele to determine the implication for biological function important in the disease. Protein structures were modeled to examine the changes in protein configuration, initially yielding four distinct groups (Figure 3) that ranged from non-abortive to variations of proteins all of which caused abortion. These alleles were directly compared to those validated in vivo and found to be linked to specific protein loops within alleles verified previously [16,22,23]—in all cases μ PathML found each of those to be biologically important for abortion and found new hybrid versions of the protein that were previously unrecognized.

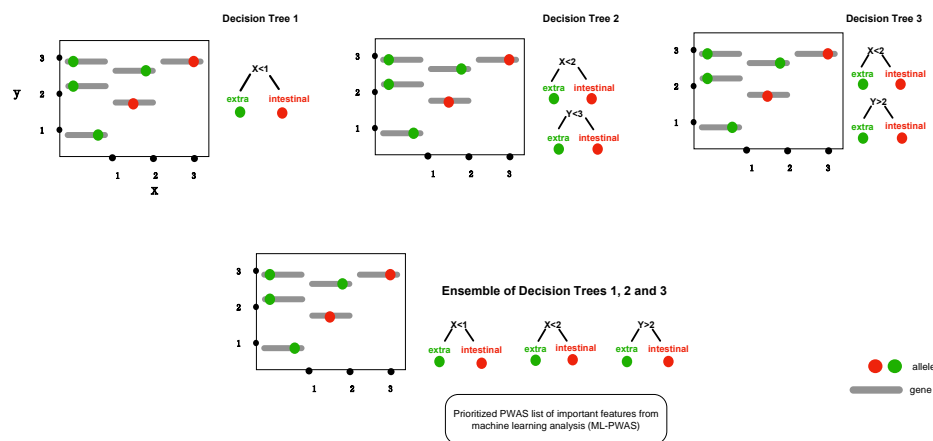


Figure 2. The conceptual framework diagram depicting machine learning in bacterial genome-wide association using extreme gradient boosting (XGBoost). Boosting is a technique of combining a set of weak classifiers or decision trees to increase prediction accuracy. Red dots represent an allelic variant, each grey bar represents a unique allele. Individual decision trees (1, 2, 3) fail to fully capture the allelic variants associated with the phenotype (e.g., extraintestinal abortion), but combining the trees together results in a process called boosting as it increases the discriminative power.

Further verification of the approach found that each of the top-ranked alleles were located in loops 1, 3, 4, 7, which perfectly verifies the published observations using genetic manipulation and a model infection [16,22,23]. By examining every genome from abortion cases, we found variants that were between 90% identical with >75% protein homology that were designated as non-prototypical variants because the sequence variation was high enough to change protein structures but within the parameters used for automated gene calling. In a limited set of alleles, the *porA* gene was so divergent that they were missed using automated gene calling but were recovered with manual curation of the μ PathML output. Recovery of these genes created a third group of rare variant alleles that also caused abortion (Figure 4; protein homology <75%). This result provides a foundation for functional variation of a core gene from all *Campylobacter* and further provides insight into the variability of *porA* as a virulence factor, even in highly divergent alleles.

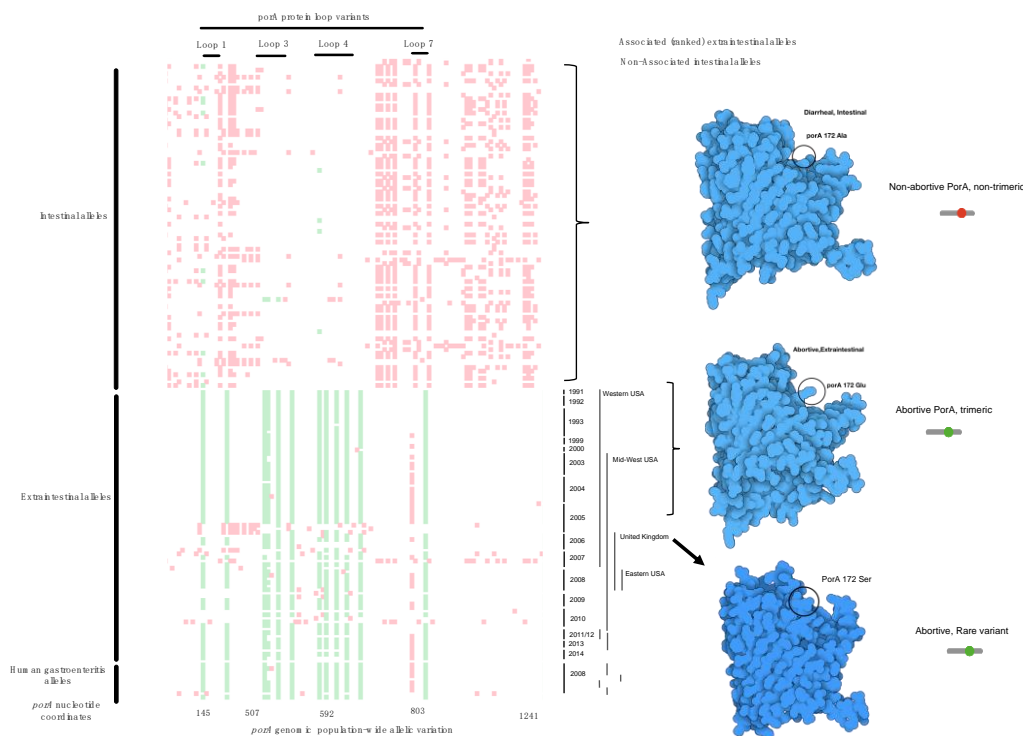


Figure 3. Comparative plot of SNP loci along the *porA* gene in all genomes. We termed this a Tetrax plot as an alternative visualization of genome-wide association hits because they are ranked and display only the loci that vary to produce a non-synonymous mutation. The *y*-axis contains individual genomes from the cases and the controls, while the *x*-axis contains the GWAS SNP loci (green), the non-disease-associated SNPs (red), open space (white) are loci that are identical in the gene sequence. Temporal and geographic metadata on the right side of the Tetrax plot provides context for mutational enrichment over 30 years and multiple distant locations in North America and the UK. The enriched SNP variation produced different protein structures (far right in blue) as the corresponding protein model by location within the animal by SNP. Protein structural features corresponding to the ranked GWAS variants are annotated on top, and below the plot are the nucleotide coordinates. Rare variants (homology <75%) were not included by the variant caller in this visualization, but manual inspection provided a method to find these variants.

All of the variants were mapped to the whole-genome phylogeny to determine whether the alleles were co-evolving at the same rate with the genome population (Figure 4). While some of the alleles were associated with similar genomes, most of the alleles were found in >2 strain genotypes. Prototypical allelic variants clustered in the largest genomic group of abortive isolates, as did some of the non-prototypical *porA* variants. However, there was significant genome variation among the population where the *porA* alleles were distributed among the genome population. Rare *porA* variants were distributed within different genomic groups and over a 15-year span between North America and the UK. The extensive allelic variation of *porA*, as well as the different genotypes, indicates that a genome surveillance system based on SNPs or a small number of genes would result in false negatives, and attempts to link these genomes to an outbreak would be unsuccessful. In combination, these observations indicate that μ PathML produced a ranked list of biologically important alleles that were validated with those that were previously shown to be causal in abortion for the exact SNP and the protein loop location. Together, these observations verified that μ PathML was capable of accurately identifying the exact SNPs in *porA* that cause abortion.

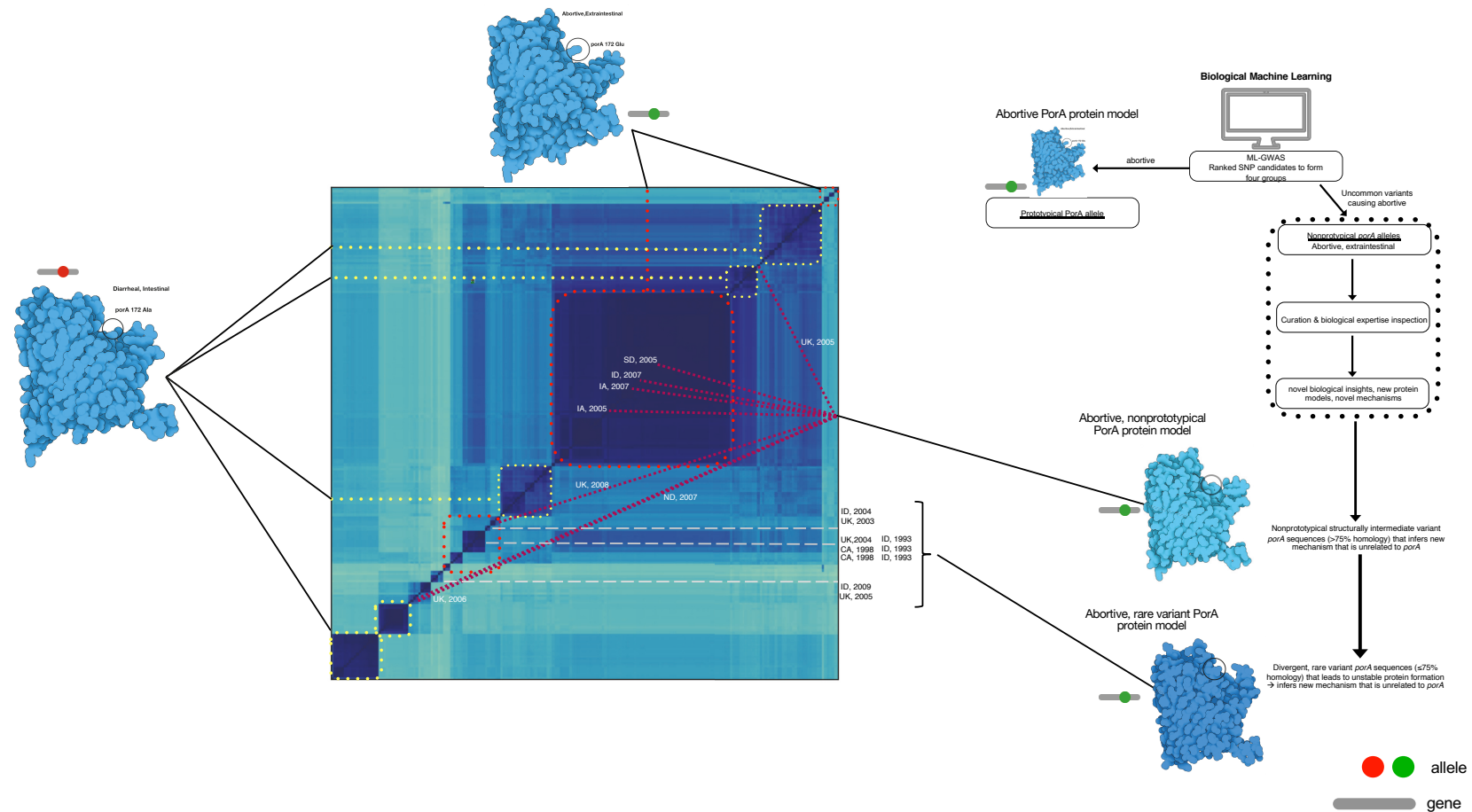


Figure 4. Whole-genome distance matrix using MinHash depicting an all-against-all comparison of genome diversity for all isolates used in this study overlaid with the *porA* variant associated with body location and disease phenotype. Genotypes and *porA* alleles are connected in this depiction to examine the association between intestinal/diarrheal location (yellow dot boxes), prototypical extraintestinal/abortive (red dot boxes), non-prototypical *porA* alleles in extraintestinal/abortive (maroon lines), and rare *porA* variants in extraintestinal/abortive (grey dashed lines) were co-located to their respective genomes in the genotype map. For the non-prototypical variants, the year and location of isolation was included to depict the variation over time and space in the maintenance of a minority population of *porA* alleles of extraintestinal abortive *C. jejuni*. The diagram to the right depicts the process used for this analysis.

4. Discussion

Since each μ PathML allele was accurately validated for accuracy to empirical studies based on animal models and genetic evidence, we broadened the examination of the protein changes from the ranked alleles to determine whether the protein structure variation contained a specific feature or amino acid substitution that was linked to abortion (Figure 5). The first six top-ranked alleles contained various amino acid substitutions for each *porA* sequence and multiple PorA protein models. However, Lys₁₈₉ was conserved among the extraintestinal *porA* allele and Asn₁₈₉ was found in the intestinal alleles. Lys mutation changes are the most impactful in membrane pore structure and are one of the tenets of membrane topology as the positive inside rule [27,28]. The positive inside rule describes the observation across membrane pores that associate positively charged amino acids within the cytoplasm and negatively charged amino acids in the extracellular domain. Membrane topology can radically change from being oriented inside the membrane (exposed to the periplasm in this case) to outside the membrane with a single Lys₁₈₉ mutation, suggesting that this mutation may flip the protein orientation in the membrane relative to Asn. Within the adjacent protein structure, Lys snorkeling effectively minimized the non-polar chain component by burying it in the hydrophobic domain and at the same time exposed the polar component to the aqueous domain, another single amino acid change that alters the topology of the membrane domain [29]. Bacterial membrane pore flipping could be a potential mechanism to avoid recognition by the immune system and enhance of ion transport for bacterial metabolism. In atypical (i.e., hypervariable alleles) this position is buried in a deeper position due to insertional mutation in rare variants, the inserted amino acids contain Lys₁₉₇, a new mutational position as compared to the prototypical protein model. Additionally, insertions in the rare variants reduce the homology to <75% leading to more extensive protein structural changes, as expected, that changed the PorA protein orientation in the membrane and retained the abortive phenotype. This situation is troublesome for traditional homology approaches and would be missed completely using comparative genomics alone. However, μ PathML combined with biological tracing effectively identified this situation to successfully link multiple genotypes, protein structural models, and the disease to provide a validated basis that presents multiple underlying mechanisms for the abortive phenotype. Importantly, this finding highlights the need to examine genes and their alleles to determine causality. In this case, the role of *porA* has been controversial [30] in causing disease, and it is likely linked to the specific allele that is present and not just to the gene.

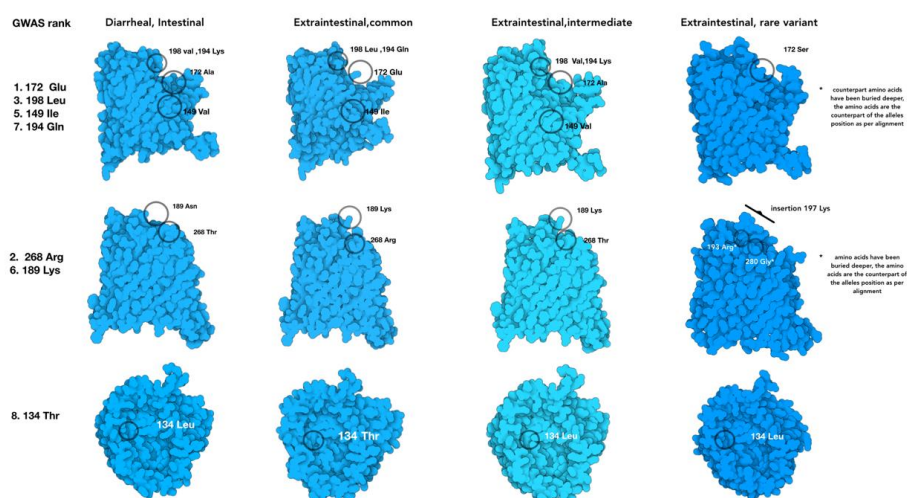


Figure 5. Protein models of the four groups of *porA* allelic variants that change the PorA protein model structure relative to the isolate location in the host and the disease outcome. The amino acids corresponding with the BioML top-ranked alleles are labeled in the common variant of PorA, while the rest show the substituted amino acid in their respective position.

5. Conclusions

This study utilized a combination of GWAS, population bacterial genomics, and machine learning to identify and rank allelic variants that correspond to biologically validated alleles of *porA* that cause abortion. The μ PathML analysis was further supported by the longitudinal and spatial conservation of the *porA* gene coupled to protein substitutions that led to important and biologically relevant changes in the structure to change activity that was linked to allelic variation conserved over 30 years and multiple global locations. A Tetris-plot visualization provided an avenue to discover divergent and rare variants that provided further insight with protein modeling that uncovered protein substitutions resulting in localization changes that affect activity and isolation localization in the host. Together these results demonstrate and validate a novel method, μ PathML, to discover biological variation combined with established mechanisms using population bacterial genomics. This approach provides an avenue to leverage the massive amount of bacterial genomic sequences to uncover new mechanisms of disease with potential to provide therapeutic approaches.

Supplementary Materials: The following are available online at <http://www.mdpi.com/2076-2607/8/4/549/s1>, Table SRanked allelic variants using BioML. Table SMetadata for extraintestinal *Campylobacter jejuni*. Table SMetadata for intestinal *Campylobacter jejuni*. Table SConfusion matrix and derived model metrics for the XGBoost model with extraintestinal *Campylobacter jejuni*. TP = true positive, FN = false negative, FP = false positive, FN = false negative.

Author Contributions: Conceptualization, DJD.D.R.B. and B.C.W.; methodology, DJD.D.R.B. and B.C.W.; software, DJD.D.R.B.; validation DJD.D.R.B. and B.C.W.; formal analysis, DJD.D.R.B. and B.C.W.; investigation, D.D.B.; resources, B.C.W.; data curation, DJD.D.R.B.; writing—original draft preparation, DJD.D.R.B.; writing—review and editing, B.C.W.; visualization, DJD.D.R.B.; supervision, B.C.W.; project administration, DJD.D.R.B.; funding acquisition, B.C.W. All authors have read and agreed to the published version of the manuscript.

Funding: DJD.D.R.B. is grateful for the funding provided by the CHED-Philippine California Advanced Research Institute to fund his PhD program.

Conflicts of Interest: The authors declare no conflict of interest. The funders had no role in the design of the study; in the collection, analyses, or interpretation of data; in the writing of the manuscript; or in the decision to publish the results.

References

- Page, A.; Cummins, C.; Hunt, M.; Wong, V.K.; Reuter, S.; Holden, M.T.; Fookes, M.; Falush, D.; Keane, J.A.; Parkhill, J. Roary: rapid large-scale prokaryote pan genome analysis. *Bioinformatics* **2015**, *31*, 3691–3693. [[CrossRef](#)] [[PubMed](#)]
- Power, R.; Parkhill, J.; De Oliveira, T. Microbial genome-wide association studies: lessons from human GWAS. *Nat. Rev. Genet.* **2016**, *18*, 41–50. [[CrossRef](#)] [[PubMed](#)]
- Johnson, R.; Nelson, G.W.; Troyer, J.L.; A Lautenberger, J.; Kessing, B.; Winkler, C.A.; O'Brien, S.J. Accounting for multiple comparisons in a genome-wide association study (GWAS). *BMC Genomics* **2010**, *11*, 724. [[CrossRef](#)] [[PubMed](#)]
- Weimer, B.C.; Storey, D.B.; Elkins, C.A.; Baker, R.C.; Markwell, P.; Chambliss, D.D.; Edlund, S.B.; Kaufman, J. Defining the food microbiome for authentication, safety, and process management. *IBM J. Res. Dev.* **2016**, *60*, 1:1–1:13. [[CrossRef](#)]
- Kaufman, J.H.; Elkins, C.A.; Davis, M.; Weis, A.M.; Huang, B.C.; Mammel, M.K.; Patel, I.R.; Beck, K.L.; Edlund, S.; Chambliss, D.; et al. Insular Microbiogeography: Three Pathogens as Exemplars. *Curr. Issues Mol. Boil.* **2019**, *36*, 89–108.
- Kaufman, J.H.; Seabolt, E.; Kunitomi, M.; Agarwal, A.; Beck, K.; Krishnareddy, H.; Weimer, B.C. Exploiting Functional Context in Biology: Reconsidering Classification of Bacterial Life. *2018 IEEE 34th Int. Conf. Data Eng. Workshops (ICDEW)* **2018**, *2018*, 17–20.
- Kaufman, J.H.; Christopher, A.E.; Matthew, D.; Allison, M.W.; Bihua, C.H.; Mark, K.M.; Isha, R.; Patel, K.L.; Beck, S.E.; David, C.; et al. Microbiogeography and microbial genome evolution. *arXiv* **2017**, arXiv:1703.07454.
- Breiman, L. Statistical Modeling: The Two Cultures (with comments and a rejoinder by the author). *Stat. Sci.* **2001**, *16*, 199–231. [[CrossRef](#)]

9. Draper, J.; Hansen, L.M.; Bernick, D.L.; Abedrabbo, S.; Underwood, J.G.; Kong, N.; Huang, B.C.; Weis, A.; Weimer, B.C.; Van Vliet, A.H.M.; et al. Fallacy of the Unique Genome: Sequence Diversity within Single *Helicobacter pylori* Strains. *mBio* **2017**, *8*, e02321-16. [[CrossRef](#)]
10. Heithoff, D.M.; Shimp, W.R.; House, J.K.; Xie, Y.; Weimer, B.C.; Sinsheimer, R.L.; Mahan, M.J. Intraspecies Variation in the Emergence of Hyperinfectious Bacterial Strains in Nature. *PLoS Pathog.* **2012**, *8*, e1002647. [[CrossRef](#)]
11. Read, T.D.; Massey, R.C. Characterizing the genetic basis of bacterial phenotypes using genome-wide association studies: a new direction for bacteriology. *Genome Med.* **2014**, *6*, 1063. [[CrossRef](#)] [[PubMed](#)]
12. Shapiro, B.J.; Friedman, J.; Cordero, O.X.; Preheim, S.P.; Timberlake, S.C.; Szabó, G.; Polz, M.F.; Alm, E.J. Population Genomics of Early Events in the Ecological Differentiation of Bacteria. *Science* **2012**, *336*, 48–51. [[CrossRef](#)]
13. Land, M.; Hauser, L.; Jun, S.-R.; Nookaew, I.; Leuze, M.R.; Ahn, T.-H.; Karpinets, T.; Lund, O.; Kora, G.; Wassenaar, T.M.; et al. Insights from 20 years of bacterial genome sequencing. *Funct. Integr. Genomics* **2015**, *15*, 141–161. [[CrossRef](#)] [[PubMed](#)]
14. Bobay, L.-M.; Ochman, H. The Evolution of Bacterial Genome Architecture. *Front. Genet.* **2017**, *8*, 72. [[CrossRef](#)] [[PubMed](#)]
15. Martinez-Carranza, E.; Barajas, H.; Alcaraz, L.D.; Servin-Gonzalez, L.; Ponce-Soto, G.Y. Variability of Bacterial Essential Genes Among Closely Related Bacteria: The Case of *Escherichia coli*. *Front. Microbiol.* **2018**, *9*, 1059. [[CrossRef](#)] [[PubMed](#)]
16. Wu, Z.; Periaswamy, B.; Sahin, O.; Yaeger, M.; Plummer, P.; Zhai, W.; Shen, Z.; Dai, L.; Chen, S.L.; Zhang, Q. Point mutations in the major outer membrane protein drive hypervirulence of a rapidly expanding clone of *Campylobacter jejuni*. *Proc. Natl. Acad. Sci. USA* **2016**, *113*, 10690–10695. [[CrossRef](#)]
17. Seemann, T. Prokka: rapid prokaryotic genome annotation. *Bioinformatics* **2014**, *30*, 2068–2069. [[CrossRef](#)]
18. Bandoy, D.D. Pangenome guided pharmacophore modelling of enterohemorrhagic *Escherichia coli* sdiA. *F1000Research* **2019**, *8*, 33. [[CrossRef](#)]
19. Brown, C.T.; Irber, L. sourmash: a library for MinHash sketching of DNA. *J. Open Source Softw.* **2016**, *1*, 27. [[CrossRef](#)]
20. Waterhouse, A.; Bertoni, M.; Bienert, S.; Studer, G.; Tauriello, G.; Gumienny, R.; Heer, F.T.; Beer, T.A.P.D.; Rempfer, C.; Bordoli, L.; et al. SWISS-MODEL: homology modelling of protein structures and complexes. *Nucleic Acids Res.* **2018**, *46*, W296–W303. [[CrossRef](#)]
21. Bienert, S.; Waterhouse, A.; De Beer, T.; Tauriello, G.; Studer, G.; Bordoli, L.; Schwede, T. The SWISS-MODEL Repository—new features and functionality. *Nucleic Acids Res.* **2016**, *45*, D313–D319. [[CrossRef](#)] [[PubMed](#)]
22. Weis, A.; Clothier, K.A.; Huang, B.C.; Kong, N.; Weimer, B.C. Draft Genome Sequences of *Campylobacter jejuni* Strains That Cause Abortion in Livestock. *Genome Announc.* **2016**, *4*, e01324-16. [[CrossRef](#)] [[PubMed](#)]
23. Weis, A.; Storey, D.B.; Taff, C.C.; Townsend, A.K.; Huang, B.C.; Kong, N.T.; Clothier, K.A.; Spinner, A.; Byrne, B.A.; Weimer, B.C. Genomic Comparison of *Campylobacter* spp. and Their Potential for Zoonotic Transmission between Birds, Primates, and Livestock. *Appl. Environ. Microbiol.* **2016**, *82*, 7165–7175. [[CrossRef](#)] [[PubMed](#)]
24. Chen, T.; Guestrin, C. XGBoost. In Proceedings of the 22nd ACM SIGKDD International Conference on Knowledge Discovery and Data Mining - KDD, San Francisco, CA, USA, 13–17 August 2016; Association for Computing Machinery (ACM): New York, NY, USA, 2016; pp. 785–794.
25. Behravan, H.; Hartikainen, J.M.; Tengström, M.; Pylkäs, K.; Winqvist, R.; Kosma, V.; Mannermaa, A. Machine learning identifies interacting genetic variants contributing to breast cancer risk: A case study in Finnish cases and controls. *Sci. Rep.* **2018**, *8*, 13149. [[CrossRef](#)]
26. Yang, J.; Wright, S.N.; Hamblin, M.; McCloskey, U.; Alcantar, M.A.; Schrübbbers, L.; Lopatkin, A.J.; Satish, S.; Nili, A.; Palsson, B.O.; et al. A White-Box Machine Learning Approach for Revealing Antibiotic Mechanisms of Action. *Cell* **2019**, *177*, 1649–1661.e9. [[CrossRef](#)]
27. Nilsson, I.; Von Heijne, G. Fine-tuning the topology of a polytopic membrane protein: Role of positively and negatively charged amino acids. *Cell* **1990**, *62*, 1135–1141. [[CrossRef](#)]
28. Elazar, A.; Weinstein, J.J.; Prilusky, J.; Fleishman, S. Interplay between hydrophobicity and the positive-inside rule in determining membrane-protein topology. *Proc. Natl. Acad. Sci. USA* **2016**, *113*, 10340–10345. [[CrossRef](#)]

29. Kim, C.; Schmidt, T.; Cho, E.-G.; Ye, F.; Ulmer, T.S.; Ginsberg, M.H. Basic amino-acid side chains regulate transmembrane integrin signalling. *Nature* **2011**, *481*, 209–213. [[CrossRef](#)] [[PubMed](#)]
30. Khan, I.; Adler, B.; Haridas, S.; Albert, M.J. PorA protein of *Campylobacter jejuni* is not a cytotoxin mediating inflammatory diarrhoea. *Microbes Infect.* **2005**, *7*, 853–859. [[CrossRef](#)]



© 2020 by the authors. Licensee MDPI, Basel, Switzerland. This article is an open access article distributed under the terms and conditions of the Creative Commons Attribution (CC BY) license (<http://creativecommons.org/licenses/by/4.0/>).